

Impact vibration properties of locally resonant fluid-conveying pipes

Bing Hu(胡兵), Fu-Lei Zhu(朱付磊), Dian-Long Yu(郁殿龙)†, Jiang-Wei Liu(刘江伟), Zhen-Fang Zhang(张振方), Jie Zhong(钟杰), and Ji-Hong Wen(温激鸿)

Citation: Chin. Phys. B, 2020, 29 (**12**): 124301. DOI: 10.1088/1674-1056/abb312
Journal homepage: http://cpb.iphy.ac.cn; http://iopscience.iop.org/cpb

What follows is a list of articles you may be interested in

Using Helmholtz resonator arrays to improve dipole transmission efficiency in waveguide

Liwei Wang(王力维), Li Quan(全力), Feng Qian(钱枫), Xiaozhou Liu(刘晓宙)
Chin. Phys. B, 2019, 28 (**9**): 094301. DOI: 10.1088/1674-1056/ab3447

Propagation of acoustic waves in a fluid-filled pipe with periodic elastic Helmholtz resonators

Dian-Long Yu(郁殿龙), Hui-Jie Shen(沈惠杰), Jiang-Wei Liu(刘江伟), Jian-Fei Yin(尹剑飞), Zhen-Fang Zhang(张振方), Ji-Hong Wen(温激鸿)
Chin. Phys. B, 2018, 27 (**6**): 064301. DOI: 10.1088/1674-1056/27/6/064301

Wave propagation in beams with anti-symmetric piezoelectric shunting arrays

Sheng-Bing Chen(陈圣兵), Gang Wang(王刚)
Chin. Phys. B, 2016, 25 (**3**): 034301. DOI: 10.1088/1674-1056/25/3/034301

Acoustic radiation from the submerged circular cylindrical shell treated with active constrained layer damping

Yuan Li-Yun, Xiang Yu, Lu Jing, Jiang Hong-Hua
Chin. Phys. B, 2015, 24 (**12**): 124301. DOI: 10.1088/1674-1056/24/12/124301

Superwide-angle acoustic propagations above the critical angles of the Snell law in liquid–solid superlattice

Zhang Sai, Zhang Yu, Gao Xiao-Wei
Chin. Phys. B, 2014, 23 (**12**): 124301. DOI: 10.1088/1674-1056/23/12/124301

Impact vibration properties of locally resonant fluid-conveying pipes*

Bing Hu(胡兵), Fu-Lei Zhu(朱付磊), Dian-Long Yu(郁殿龙)†, Jiang-Wei Liu(刘江伟), Zhen-Fang Zhang(张振方), Jie Zhong(钟杰), and Ji-Hong Wen(温激鸿)

Laboratory of Science and Technology on Integrated Logistics Support, National University of Defense Technology, Changsha 410073, *China*

(Received 22 July 2020; revised manuscript received 26 August 2020; accepted manuscript online 27 August 2020)

Fluid-conveying pipe systems are widely used in various equipments to transport matter and energy. Due to the fluid–structure interaction effect, the fluid acting on the pipe wall is easy to produce strong vibration and noise, which have a serious influence on the safety and concealment of the equipment. Based on the theory of phononic crystals, this paper studies the vibration transfer properties of a locally resonant (LR) pipe under the condition of fluid–structure interaction. The band structure and the vibration transfer properties of a finite periodic pipe are obtained by the transfer matrix method. Further, the different impact excitation and fluid–structure interaction effect on the frequency range of vibration attenuation properties of the LR pipe are mainly considered and calculated by the finite element model. The results show that the existence of a low-frequency vibration bandgap in the LR pipe can effectively suppress the vibration propagation under external impact and fluid impact excitation, and the vibration reduction frequency range is near the bandgap under the fluid–structure interaction effect. Finally, the pipe impact experiment was performed to verify the effective attenuation of the LR structure to the impact excitation, and to validate the finite element model. The research results provide a technical reference for the vibration control of the fluid-conveying pipe systems that need to consider blast load and fluid impact.

Keywords: locally resonant pipe, fluid–structure interaction, transfer matrix method, impact vibration properties

PACS: 43.40.+s, 47.35.Lf, 46.40.–f, 61.50.Ah **DOI:** 10.1088/1674-1056/abb312

1. Introduction

The fluid-conveying pipe systems are widely used in various equipments to transfer matter and energy. Due to the interaction between the pipe wall and the fluid, the pressure wave pulsation of fluid being conveyed may induce strong vibration and noise, which will affect the equipment performance.[1,2] In particular, the blast wave caused by the underwater explosion will excite strong vibrations and noises of the fluid-conveying pipe system, and cause serious damage to the pipe system and even the related equipment.[3] Besides, when the control system of the fluid-conveying pipe changes, the suddenly changed movement state of the fluid in the pipe will have a strong impact on the pipe wall, and thus may cause damage to the pipe system.[4] Therefore, it is significant in theory and practice to study how to reduce the vibration and then ensure the safety of the fluid-conveying pipe system under the condition of impact excitation.

In recent years, the continuously developing theory of the bandgap in phononic crystals (PCs) in condensed matter physics provides new technical support for vibration propagation control.[5–10] Flexural vibrations in the Timoshenko beam and Euler–Bernoulli beam with locally resonant (LR) structures were studied theoretically and experimentally by Yu *et al.*[11,12] Xiao *et al.*[13,14] extended the plane wave expansion method and studied the propagation of flexural waves in local resonance beams with multiple additional spring–mass resonators. The propagation of flexural waves in an actively controllable LR beam was theoretically studied by Zhou *et al.*[15] Chen *et al.*[16–18] studied the sandwich beam structure with internal LR, and the results show that it can improve the flexural vibration performance under impact load. Pai *et al.*[19] realized the effective combination of two bandgap frequency regions to form a single broadband energy absorption region by incorporating damping elements into a multi-resonator metamaterial beam. Alamri *et al.*[20] introduced the development of dissipative elastic metamaterials with multiple Maxwell resonators, which can be applied to reduce dynamic loads and attenuation of the blast wave. Li *et al.*[21,22] proposed a three-resonators metamaterial to enhance the attenuation of impact stress waves, conducted a multi-objective optimization of the metamaterial, and then proposed a new multi-resonators metamaterial for attenuation of impact stress waves. The elastic wave metamaterials with the LR have better crack resistance and show the meta-arrest property, which were studied by Wang *et al.*[23] From theoretical research to practical applications, the above researches have made a lot of progress on the bandgap and wave attenuation properties of the PCs. However, most of the research works consider the vibration of solid structures, few researches focus on the related characteristics under fluid–structure interaction effect.

*Project supported by the National Natural Science Foundation of China (Grant No. 11872371) and Major Program of the National Natural Science Foundation of China (Grant Nos. 11991032 and 11991034).

†Corresponding author. E-mail: dianlongyu@vip.sina.com

© 2020 Chinese Physical Society and IOP Publishing Ltd

Usually, there are two paths for utilizing the bandgap properties of the PCs to suppress the vibration propagation of the pipe system. One is to design the pipe system as a periodic composite structure;[24] the other is to periodically attach local resonance along the pipe. Both paths provide new technical approaches for the design of vibration and noise reduction in the pipe system, and have been widely studied and paid attention to.[25–33] Sorokin *et al.*[34] studied the coupling vibration bandgap of the longitudinal vibration and flexural vibration of a pipe with a periodically added inertial mass system. Wang *et al.*[35] studied the effects of the viscous fluid on the propagation characteristics of elastic waves in carbon nanotubes based on the nonlocal continuum theory and the small scales effects were also considered. Yu *et al.*[36] realized the flexural vibration bandgap of a periodic composite fluid-conveying pipe by applying Bragg scattering mechanism and local resonance mechanism, further studied the wave propagation and attenuation properties of the fluid-conveying pipe under various conditions,[37–41] and conducted vibration tests to verify the wave attenuation capability of the periodic pipe structure.[42] Based on the shell model, Shen *et al.*[43] focused on the bandgap formation mechanism and vibration properties of the local resonance fluid-conveying pipe, and analyzed the influences of various parameters and boundary conditions. Iqbal *et al.*[44] studied the band structure and vibration transfer properties of the pipe system with lateral localized and laterally distributed resonators based on the PC pipe model. The above researches have laid a foundation for the vibration analysis of the PC fluid-conveying pipe. However, less consideration has been given to the fluid–structure interaction effect in these studies. Especially, the vibration analysis of impact excitation is not deeply enough studied.

In this paper, the LR fluid-conveying pipe which has the fluid–structure interaction effect will be taken as the object, and the influence of different impact excitation conditions on the vibration properties will be mainly considered. Based on the transfer matrix method, vibration transfer properties of the LR fluid-conveying pipe are studied, the bandgap properties and vibration attenuation effects are analyzed. Further, the finite element method is used to calculate the vibration properties of the LR fluid-conveying pipe under different impact excitation and fluid–structure interaction effect. Finally, we perform impact experiments to verify the transfer matrix method and the finite element model, and to demonstrate the advantage of the LR fluid-conveying pipe for the control of pipe vibration under different impact excitation experimentally. The research results provide a technical reference for the vibration control of the fluid-conveying pipe systems that need to consider blast load and fluid impact.

2. Bandgap properties

2.1. Transfer matrix method

Vibration modes of fluid-conveying pipe include flexural vibration, axial vibration, torsional vibration, and complex coupling vibration among them. When the inner fluid flows at a higher or slower velocity, the pipe may be flexural or vibrate strongly, and under external excitation, the pipe will mainly produce flexural vibration, axial vibration, and torsional vibration which are small and can be ignored. Therefore, pipe flexural vibration is the main vibration mode.[45,46] Therefore, the study of flexural vibration has important theoretical significance for pipe vibration control. At present, most of the theoretical research on the flexural vibration of the pipe is based on the beam model.

In general, when the ratio of pipe length to pipe diameter is greater than or equal to 10, the pipe can be considered as the Euler–Bernoulli beam model.[47] Assuming that the fluid in the pipe is ideal (isotropic, uniform, incompressible, and linear), the fluid velocity is at a constant speed, cavitation does not occur in the fluid, and the influence of gravity is ignored. The Euler–Bernoulli beam equation of flexural vibration of the fluid-conveying pipe is[48–50]

$$EI\frac{\partial^4 w}{\partial x^4}+m_{\mathrm{f}}u^2\frac{\partial^2 w}{\partial x^2}+2m_{\mathrm{f}}u\frac{\partial^2 w}{\partial x\partial t}+(m_{\mathrm{f}}+m_{\mathrm{p}})\frac{\partial^2 w}{\partial t^2}=0, \quad (1)$$

where E is Young's modulus of the pipe material, I is the rotational inertia of the pipe crosssection, w is the flexural vibration displacement, m_{f} is the fluid mass per unit length, m_{p} is the pipe mass per unit length, u is the constant uniform fluid velocity, and t is time.

For a harmonic traveling wave,[47] the solution of Eq. (1) can be written as the form of $w(x,t)=W\mathrm{e}^{kx}\mathrm{e}^{\mathrm{i}\omega t}$, then the flexural vibration equation of the pipe can be described by

$$EIk^4+m_{\mathrm{f}}u^2k^2+\mathrm{i}2m_{\mathrm{f}}u\omega k-(m_{\mathrm{f}}+m_{\mathrm{p}})\omega^2=0. \quad (2)$$

For a given ω, the wavenumber k in Eq. (2) has two different imaginary roots and two complex roots that are conjugated to each other. By denoting the four roots of k as k_1, k_2, k_3, k_4, then the solution of Eq. (1) can be described as follows:

$$\omega(x,t)=\mathrm{e}^{\mathrm{i}\omega t}\left(W_1\mathrm{e}^{k_1x}+W_2\mathrm{e}^{k_2x}+W_3\mathrm{e}^{k_3x}+W_4\mathrm{e}^{k_4x}\right). \quad (3)$$

We have designed a LR fluid-conveying pipe. Its structural sketch is shown in Fig. 1. The selected local resonator is composed of a rubber ring and a metal ring. The rubber ring is wrapped on the outside of the pipe wall. The equivalent physical model of the LR is the spring–mass model. Where a is the length of the periodic pipe cell, i.e., the lattice constant, l is the length of the local resonator, r_0 and r_1 are the inner diameter and outer diameter of the main pipe, respectively, r_2 and

r_3 are the outer diameters of the rubber ring and metal ring, respectively.

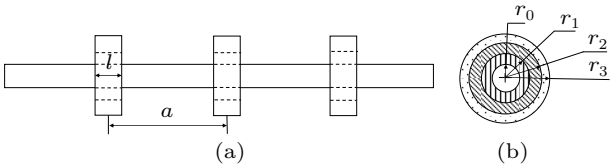


Fig. 1. (a) A sketch of the LR fluid-conveying pipe, (b) a LR structure.

When the material damping of the rubber ring is not considered, the local resonator can be equivalent to a spring–mass model, and its structure diagram is shown in Fig. 2.

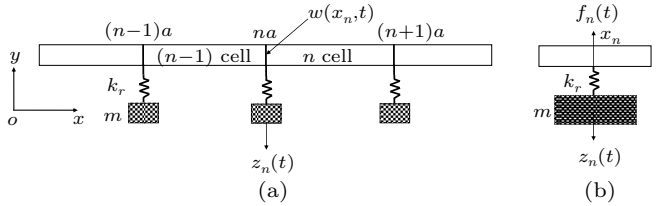


Fig. 2. (a) Equivalent model of the LR fluid-conveying pipe, (b) equivalent model of a single cell.

For the n^{th} local resonator, according to the force analysis, it can be see that[11]

$$f_n(t) - m\ddot{z}_n(t) = 0, \tag{4}$$

where $f_n(t)$ is the shear force of the local resonator on the pipe at x_n, $z_n(t) = Z_n \exp(\mathrm{i}\omega t)$ is the displacement of the n^{th} oscillator, and Z_n is the amplitude of the n^{th} oscillator. f_n can be described as

$$\begin{aligned} f_n(t) &= k_r[w(x_n,t) - z_n(t)] \\ &= k_r[w(0) - Z_n]\exp(\mathrm{i}\omega t) = F_n \exp(\mathrm{i}\omega t). \end{aligned} \tag{5}$$

Substituting Eq. (5) into Eq. (4) leads to

$$Z_n = \frac{k_r}{k_r - m\omega^2} w_n(0), \tag{6}$$

where k_r is the equivalent radial stiffness of the rubber ring and m is the mass of the local resonator.

The displacement, slope, bending moment, and shear force at the interface between cell $n-1$ and cell n are all continuous. Following the transfer matrix method and Bloch's theorem, the eigenvalues of an infinite periodic fluid-conveying pipe structure is the root of the determinant

$$\left| \boldsymbol{T} - \mathrm{e}^{\mathrm{i}qa} \boldsymbol{I} \right| = 0, \tag{7}$$

where $\boldsymbol{I}$ is the 4×4 unit matrix and q is the one-dimensional wave vector in the x direction. For a given value of ω, equation (7) gives the corresponding value of q. Depending on whether q is a real or imaginary component, the corresponding wave propagates through the fluid-conveying pipe (passband) or is damped (bandgap).

For a pipe with n finite periodic cells, the frequency response curve can be obtained from the transfer matrix $\boldsymbol{T}$ to describe its bandgap properties, and we obtain[47]

$$\boldsymbol{W}_n = \boldsymbol{T}^n \boldsymbol{W}_0. \tag{8}$$

2.2. Bandgap properties of LR fluid-conveying pipes

In the calculation, the materials of the main pipe, the rubber ring, and metal ring of the LR are steel, rubber, and copper, respectively. The related values of the geometric and material parameters are shown in Tables 1 and 2. The medium in the pipe is water, with density 1000 kg/m^3 and the sound velocity 1400 m/s. The band structure diagram of the infinite period cell is calculated under the above parameters.

Table 1. Geometric parameters of the pipe (unit: m).

a	l	r_0	r_1	r_2	r_3
0.5	0.1	0.04	0.045	0.06	0.08

Table 2. Material parameters of the pipe.

	Young's modulus/Pa	Density/(kg/m^3)	Poisson's ratio	Shear modulus/Pa
Steel	2×10^{11}	7850	0.3	7.7×10^{10}
Rubber	5.9×10^6	1300	0.49	2×10^6
Copper	8×10^{11}	8950	0.3	3×10^{11}

For the LR cell, due to the small length of the rubber ring, it can be regarded as a uniform force when the radial force is applied, and its equivalent radial stiffness is[11]

$$k_r = \frac{\pi\left(5 + 3.29H^2\right) G_{\text{rubber}} l}{\ln(r_2/r_1)}, \tag{9}$$

where $H = \frac{l}{(r_2+r_1)\ln(r_1/r_2)}$ is the shape factor and G_{rubber} is the shear modulus of the rubber material.

Considering that the fluid velocity in the pipe is $u = 0$ m/s, the transfer matrix method is used to calculate the band structure and frequency response of the flexural vibration of the LR fluid-conveying pipe. And we mainly consider the vibration response of the pipe within 0–800 Hz. It is effectively convergent to use the transfer matrix method to calculate the frequency response within the frequency range. Figure 3(a) shows the relation curve between the real part of the wave vector and frequency. Figure 3(b) shows the frequency response curve of a LR pipe with 8 cells. It can be seen from the figure that the fluid-conveying pipe has an attenuation bandgap of 360–730 Hz in the frequency range of 0–800 Hz. From the vibration frequency response curve, it can be seen that the vibration transfer curve of the finite periodic PC pipe agrees well with the bandgap frequency range of the infinite periodic PC pipe, and the attenuation amplitude can be as low as -110 dB.

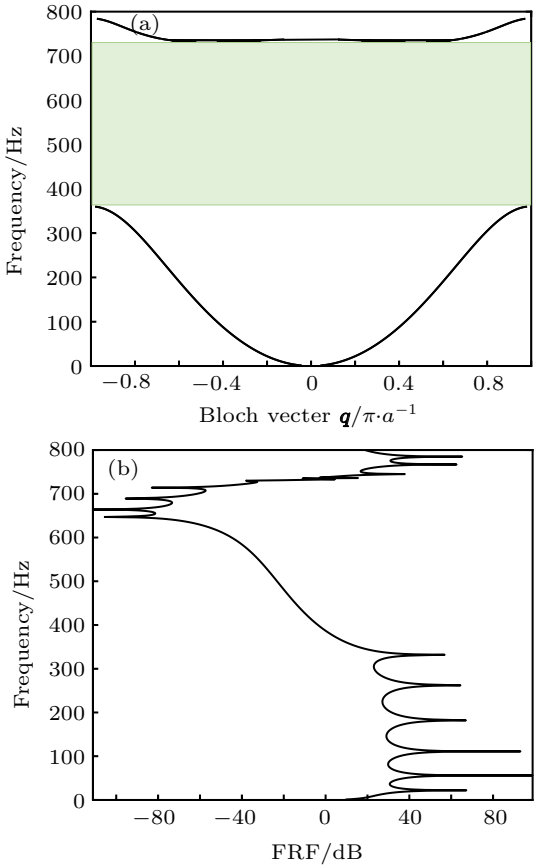


Fig. 3. Bandgap properties of LR fluid-conveying pipe: (a) band structure, (b) frequency response curve.

3. Numerical simulation of vibration properties of the LR fluid-conveying pipes

3.1. Fluid–structure interaction numerical simulation model

Considering the vibration transfer properties of the LR pipe under the condition of fluid–structure interaction, based on the ANSYS workbench, the fluid–structure interaction analysis of the LR pipe under different impact excitations is carried out, and the basic flow of the two-way fluid–structure interaction analysis is established as shown in Fig. 4. The material of the inlet and outlet pipes is the same as the material of the main pipe of the LR pipe. Refer to Fig. 1 for the structural parameters of the LR pipe, and establish a 3 cells LR pipe model as shown in Fig. 5. The model is selected as the transient structure and fluid flow module. The total length of the pipe is 3.5 m, the internal diameter of the pipe is 0.08 m, the thickness of the pipe wall is 0.005 m, and the elastic pipe wall ignores the damping effect of the pipe. The fluid part is incompressible water with density 1000 kg/m^3, water temperature 25 °C, and the dynamic viscosity coefficient 0.001003 kg/m·s. When the ANSYS workbench calculates the two-way fluid–structure interaction, the fluid transmitted through the fluid–structure interaction surface to the pipe structure is only the fluid force of the fluid Reynolds stress, viscous stress, and pulsating shear stress generated by the turbulent motion, excluding the fluid mass. Thus, in the simulation calculation, the result is more accurate for light fluids. However, when the fluid in the pipe is heavy, the simulation results will produce larger errors, and it is necessary to introduce additional mass $\Delta m = \rho\pi r_{\mathrm{p}}^2$ into the pipe. The fluid in this paper is water, which belongs to heavy fluid, therefore the equivalent density of the pipe material needs to be set when modeling the pipe,

$$\rho_{\mathrm{e}} = \rho_0 + \rho_{\mathrm{f}} \frac{r_{\mathrm{in}}^2}{r_{\mathrm{out}}^2 - r_{\mathrm{in}}^2}, \tag{10}$$

where ρ_0 is the pipe material density, ρ_{f} is the fluid density, r_{in} is the pipe inner diameter, and r_{out} is the pipe outer diameter. The material of the pipe and the local resonator material are selected from steel, rubber, and copper in Table 2. Then the equivalent density of the steel material of the main pipe set in the simulation analysis is 11614.7 kg/m^3.

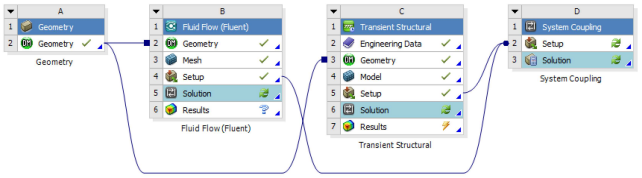


Fig. 4. Fluid–structure interaction configuration in the ANSYS workbench.

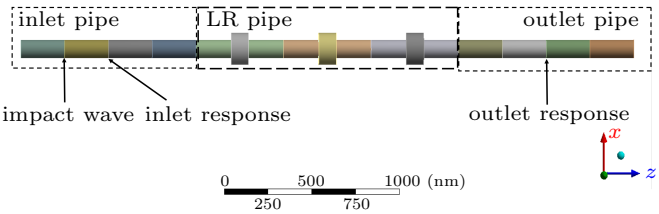


Fig. 5. Establishment of impact response model of fluid–structure interaction pipe in the ANSYS.

In this case, the inner wall surface of the pipe, where the fluid and the solid are in contact, is a fluid–structure interface, and the boundary conditions are set as fixed constraints. Set different inlet speeds in the Fluent interface, and the outlet pressure is set to 0 Pa. Set the coupling time and coupling time step as 0.0512 s and 0.0001 s, and select two-way coupling in the system coupling analysis interface.

3.2. Analysis of vibration properties of the LR fluid-conveying pipes

Harmonic response analysis of the impact response model of the fluid–structure interaction pipe is shown in Fig. 5. Applying a displacement signal with an amplitude of 1 at the excitation end, and picking up displacement signals w_{in} and w_{out} at the inlet and outlet response of the fluid-conveying pipe, the frequency response curve of the LR pipe under the condition

of two ends fixed can be calculated by $\mathrm{FRF} = 20 \times \log\left(\frac{w_{\mathrm{out}}}{w_{\mathrm{in}}}\right)$, as shown in Fig. 6. It is observed that the fluid-conveying pipe has obvious attenuation in the range of 370–730 Hz. Comparing Fig. 6 with Fig. 3, the fluid–structure interaction LR pipe with 3 cycles has significant attenuation within the bandgap of the LR fluid-conveying pipe under the boundary condition of fixed supports at both ends. It lays a theoretical foundation for further study of vibration response under external and fluid impact excitation.

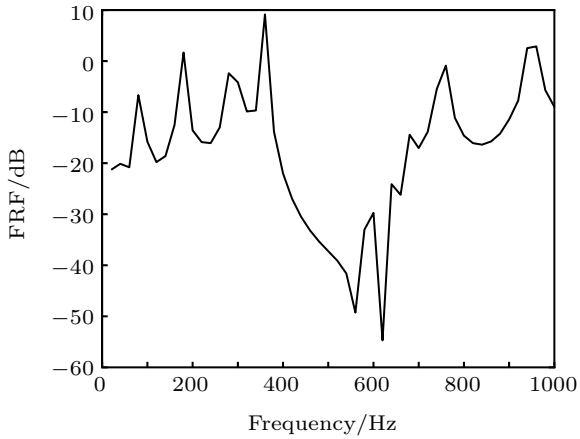


Fig. 6. Vibration transfer properties of the LR pipe with fixed ends.

4. Impact vibration properties of the LR fluid-conveying pipes

4.1. External impact excitation

Assuming that an impact load is received at 0.25 m from the left end of the pipe, which is in the radial direction at the position of the impact wave in Fig. 5. The form of the impact wave satisfies the following equation:

$$\begin{aligned} F &= F_{\max} \mathrm{e}^{-\frac{t-t_0}{t_{\mathrm{d}}}}, \quad t \geq t_0, \\ F &= 0, \qquad\qquad\quad t \leq t_0, \end{aligned} \tag{11}$$

where $F_{\max} = 200$ N, $t_0 = 0.0005$ s, $t_{\mathrm{d}} = 0.0001$ s, the impact time is 0.0005 s, and the response signal is picked up at the inlet and outlet of the pipe. The flexural vibration response of the fluid-conveying pipe is simulated and calculated. The fluid–structure interaction simulation analysis is used in the simulation analysis of the fluid-conveying pipe, and the fluid velocity is set to 0 m/s.

The impulse response of the external impact excitation is shown in Fig. 7(a), and its frequency domain distribution obtained by using the fast Fourier transform (FFT), is shown in Fig. 7(b). It can be seen that due to the effect of the external impact excitation, the stress wave generates in the model in a wide frequency band of 0–5000 Hz.

Considering the single structure pipe without additional LR and the LR fluid-conveying pipe respectively, taking the flexural vibration at the inlet and outlet of the pipe as the research object, the velocitytime curve and velocity frequency curve at inlet and outlet of the pipe are obtained through simulation analysis.

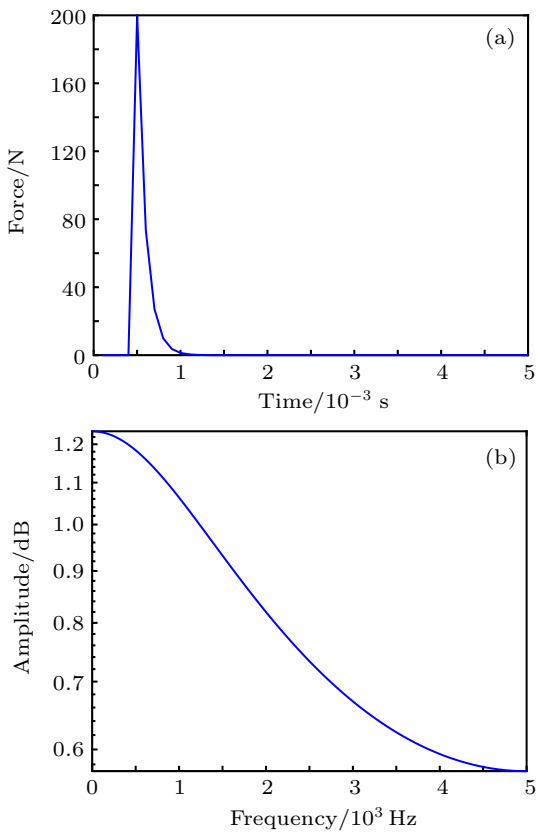


Fig. 7. (a) External impact impulse response, (b) impact simulation frequency domain obtained by fast Fourier transform.

Figure 8 shows the flexural vibration response of the single structure and LR fluid-conveying pipe under the external impact excitation, respectively. The black solid line and the blue dashed line respectively represent the velocity signal response at the inlet and outlet. The shaded part in the frequency domain diagram indicates that the velocity peak at the outlet is smaller than the velocity peak at the inlet, indicating that the LR pipe has a better attenuation effect in this frequency range. Comparing Fig. 8(a) with Fig. 8(b), it can be found that the single structure pipe basically has no attenuation effect on external impact vibration, while the LR pipe has a better attenuation effect within 490–840 Hz, which is consistent with the bandgap of the fluid-conveying pipe calculated by the finite element method in Subsection 3.2, indicating that the LR fluid-conveying pipe has a better attenuation effect on external impact.

Figure 9 represents the flexural vibration response of the inlet and outlet of the single structure and the LR fluid-conveying pipe under external impact excitation. Comparing Fig. 9(a) with Fig. 9(b), it is observed that at the inlet, the impact vibration response of the single structure and LR pipe

in the time domain and frequency domain are basically identical, but at the outlet, the amplitude of the LR pipe in the time domain is smaller than that of single structure pipe, and in the frequency domain, the amplitude of the LR pipe is significantly smaller in the bandgap range, indicating that the LR fluid-conveying pipe has significant vibration attenuation effect in a specific frequency range. The result shows that the LR pipe can effectively suppress the vibration propagation under external impact excitation, especially the vibration attenuation effect near the bandgap is better.

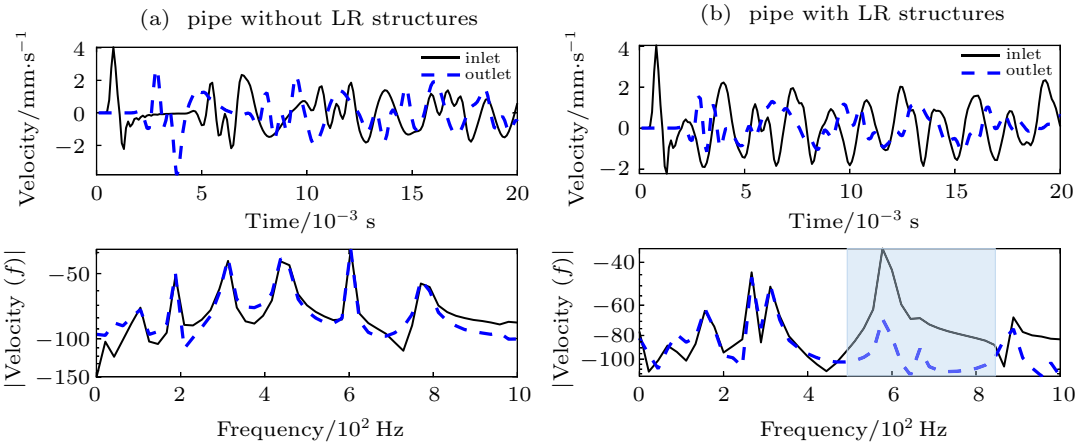


Fig. 8. Flexural vibration response of fluid-conveying pipe under external impact excitation.

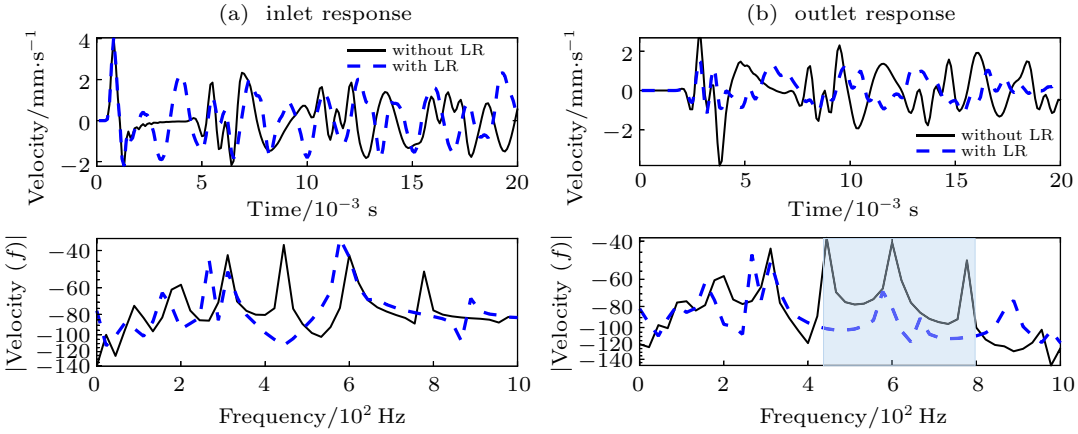


Fig. 9. Flexural vibration response of the inlet and outlet of fluid-conveying pipe under external impact excitation.

4.2. Fluid impact excitation

Assuming the initial state of the fluid velocity in the pipe is 0 m/s, when the pump or valve is opened quickly, the fluid flow changes so drastically that the fluid velocity changes accordingly. When the fluid velocity changes, the following equation is satisfied:

$$\begin{aligned} V &= V_{\max} e^{-\frac{t-t_0}{t_d}}, \quad t \geq t_0, \\ V &= 0, \qquad\qquad\quad t \leq t_0, \end{aligned} \tag{12}$$

where $V_{\max} = 50$ m/s, $t_0 = 0.0005$ s, and $t_d = 0.0001$ s. The impact time is 0.0005 s, and the response signal is picked up at the inlet and outlet of the pipe.

Considering the single structure pipe with the LR fluid-conveying pipe respectively, taking the flexural vibration at the inlet and outlet of the pipe as the research object, and the velocitytime curve and velocity frequency curve at inlet and outlet of the pipe are obtained through simulation analysis.

Figure 10 shows the flexural vibration response of a single structure and LR fluid-conveying pipe under the excitation of impact fluid. It can be found that in the time domain, the vibration response of the two pipes changes suddenly when the fluid velocity changes rapidly. With the decreases of the fluid velocity, the pipe wall vibration response decreases, the vibration at the outlet is delayed, and the vibration amplitude of the LR fluid-conveying pipe at the outlet is significantly lower than that of the single structure pipe, indicating that the LR fluid-conveying pipe has a significant attenuation effect for fluid impact vibration. The vibration response at the inlet is slightly larger than that at the outlet, which is because it takes a certain time for the fluid impact excitation to reach the outlet. In addition, the interaction effect between the fluid and the pipe wall occurs during the fluid flow, resulting in a decrease in energy and a slight decrease in the velocity at the outlet. In the frequency domain, the vibration response of

a single structure pipe at the inlet and outlet of the lowfrequency band is basically identical, but the highfrequency band is slightly attenuated after 650 Hz. This is due to the highfrequency energy attenuation caused by the fluid–structure interaction effect generated when the impacted fluid flows in the pipe. However, the LR fluid-conveying pipe attenuated in the range of 380–950 Hz, indicating that the LR fluid-conveying pipe has a significant attenuation effect on fluid impact vibration.

Further comparing the vibration response of the single structure with the LR fluid-conveying pipe at the inlet and outlet under the excitation of the impacted fluid as shown in Fig. 11, we can know that in the time domain, the vibration of the LR pipe is basically the same as the single structure pipe at the inlet. However, the peak time of the LR pipe lags behind the single structure pipe, and the amplitude is slightly smaller at the outlet, indicating that the LR pipe can effectively suppress the pipe vibration caused by fluid impact. In the frequency domain, at the inlet, the vibration amplitudes of the two types of pipes are basically identical, while at the outlet, the vibration response of the LR pipe is significantly smaller than that of the single structure pipe in 380–820 Hz, which is basically consistent to the vibration attenuation bandgap in Subsection 3.2. In summary, the LR fluid-conveying pipe can significantly attenuate the vibration of the pipe caused by fluid impact excitation. Especially, the vibration attenuation effect near the bandgap is better.

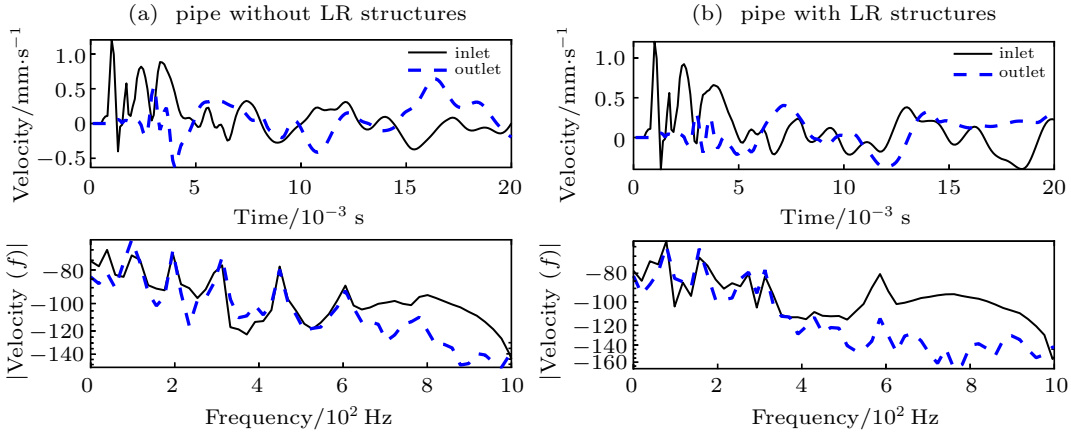


Fig. 10. Flexural vibration response of fluid-conveying pipe excited by impact fluid.

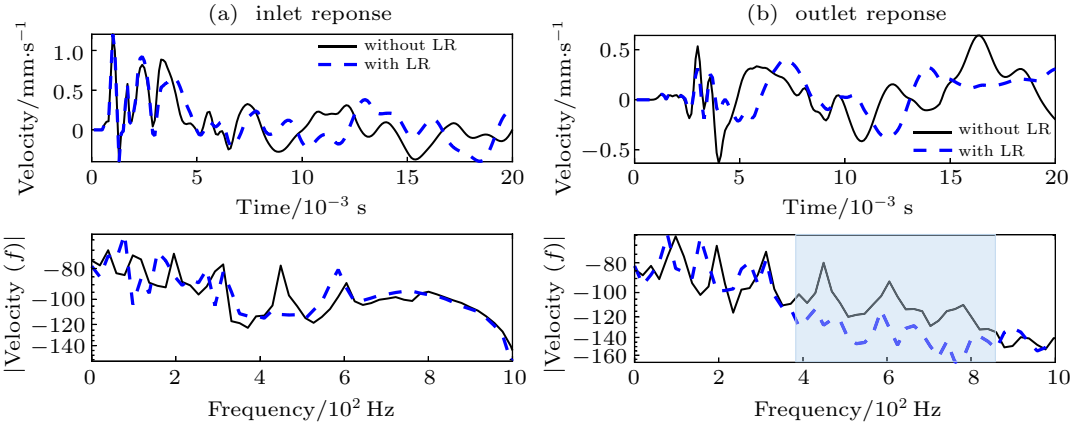


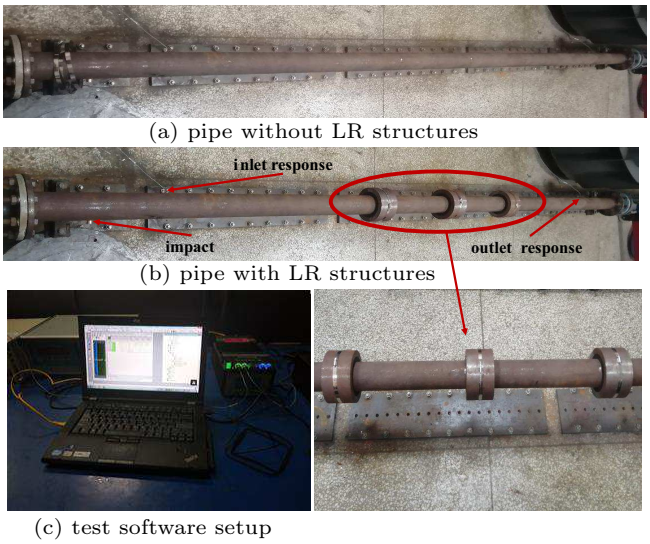
Fig. 11. Flexural vibration response of the inlet and outlet of fluid-conveying pipe excited by impact fluid.

5. Experimental validation

The pipe impact experiment is performed to verify the effective attenuation of the LR structure to the impact excitation, and to validate the finite element model in Section 4. A steel pipe with a length of 3.5 m, an inner diameter of 0.04 m, and a wall thickness of 0.005 m, three rubber rings, and copper rings with the structural parameters that are based on Table 1 are manufactured. The test piping system is built, as shown in Fig. 12, Figures 12(a)–12(c) represent a single structure pipe, a three-cycle LR pipe, a test software setup, respectively.

The impact force of the pipe wall is generated and measured by the impact hammer manually striking the excitation of the pipe, and the fluid impact is caused by the sudden opening or closing of the vertical centrifugal pump, which causes a sudden change in the fluid velocity. The vibration signal at the inlet and outlet of the pipe is picked up by two acceleration sensors B&K4507B. Then we input to the vibration signal analyzer B&K3160-B-O42. Finally, the vibration data

is collected and analyzed by the vibration analysis software B&K7700 (Pulse).



(a) pipe without LR structures

(b) pipe with LR structures

(c) test software setup

Fig. 12. The LR fluid-conveying pipe experimental setup.

Figure 13 shows the flexural vibration response of the single structure and LR fluid-conveying pipe under the excitation of the impact hammer. The black solid line and the blue dashed line respectively represent the velocity signal response at the inlet and outlet. The shaded part in the frequency domain diagram indicates that the velocity peak at the outlet is smaller than the velocity peak at the inlet, indicating that the LR pipe has a better attenuation effect in this frequency range. Comparing Fig. 13(a) with Fig. 13(b), the single structure pipe has basically no attenuation effect on the impact vibration of the pipe wall, while the LR pipe can have a good attenuation effect in 400–720 Hz, which is consistent with the attenuation bands of 490–840 Hz in Subsection 4.1. This phenomenon verifies the correctness of the finite element simulation analysis of the LR fluid-conveying pipe under external impact excitation, and shows that the LR fluid-conveying pipe has a better attenuation effect under external impact vibration.

Figure 14 shows the flexural vibration response of the single structure and LR fluid-conveying pipe at the inlet and outlet under the fluid impact excitation. Comparing Fig. 14(a) with Fig. 14(b), the single structure pipe has basically no attenuation effect on fluid impact vibration, but the LR pipe can have a better attenuation effect in the range of 490–830 Hz, which is consistent with the attenuation bands of 380–820 Hz in Subsection 4.2, indicating that the LR fluid-conveying pipe also has a better attenuation effect on fluid impact vibration. This phenomenon verifies the correctness of the finite element simulation analysis of the LR fluid-conveying pipe under fluid impact excitation.

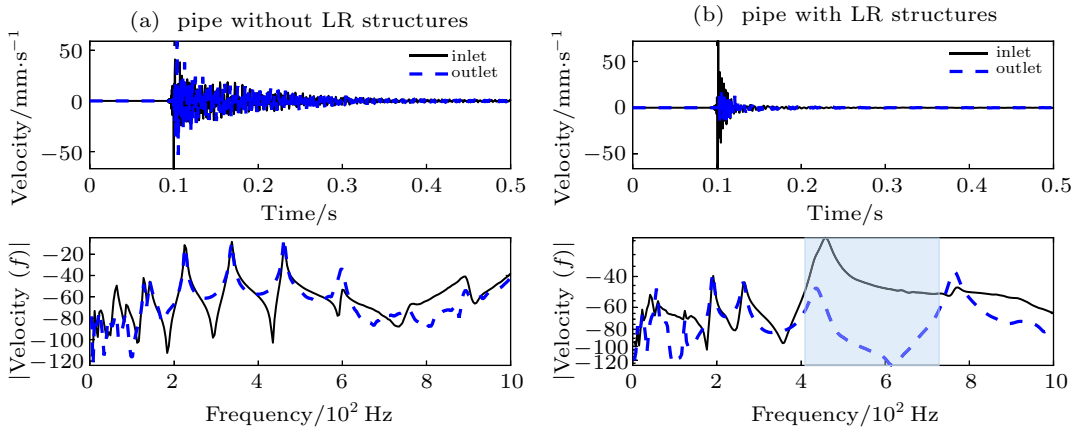


Fig. 13. Flexural vibration response of fluid-conveying pipe under external impact excitation.

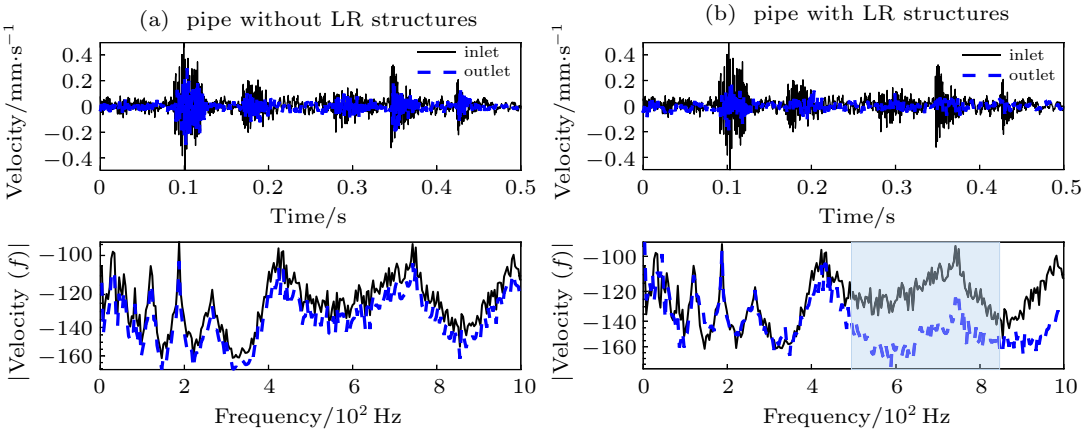


Fig. 14. Flexural vibration response of fluid-conveying pipe under fluid impact excitation.

We noticed that there are some differences between numerical simulations and experiments. The important difference between the two is that the numerical simulation analysis ignores the damping. The LR fluid-conveying pipe is a complex system with a variety of damping sources and nonlinear sources. These factors are difficult to consider in numerical simulation. On the other hand, the boundary conditions used in the experiment are not completely consistent with the numerical simulation analysis. In the experiment, the flange is used to fix the test pipe to both ends of the pipe system to simulate the fixed constraints at both ends of the test pipe, but in fact, the boundary conditions are much more complicated than the fixed constraints, which leads to the deviation of the impact wave reflection from the prediction of the fixed constraints.

6. Conclusion

In conclusion, the vibration properties of the LR fluid-conveying pipe are analyzed in this paper, focusing on the vibration properties under impact conditions. Through the research in this research, the following conclusions are drawn.

(1) Based on the Euler–Bernoulli beam model, the transfer matrix method is used to establish the bandgap properties of the calculation model of the LR fluid-conveying pipe system, which provides an effective tool for the vibration response analysis of the LR fluid-conveying pipe.

(2) The finite element model shows that the LR fluid-conveying pipe has a significant attenuation effect on the pipe vibration caused by external impact excitation and fluid impact excitation in the bandgap, indicating that when considering the fluid–structure interaction effect, the LR fluid-conveying pipe can better achieve the control of pipe vibration.

(3) The results of numerical calculation and simulation analysis are verified by external impact and fluid impact experiments, and the effectiveness of the LR fluid-conveying pipe is verified. The experimental results are in good agreement with the calculation and simulation results. Therefore, the LR fluid-conveying pipe can be used to attenuate the impact load and apply to various pipe systems that need to consider blast load and fluid impact.

References

[1] Keramat A, Tijsseling A S, Hou Q and Ahmadi A 2012 *J. Fluid Structure* **28** 434
[2] Ferràs D, Manso P A, Schleiss A J and Covas D I C 2016 *Comput. Struct.* **175** 74
[3] Jia Z Z, Ye Q, Liu W, Lu Y, Wu T R, Yang Z H and Zhu S F 2018 *Procedia Engineering* **211** 288
[4] Mahmoodi R, Zolfaghari A and Minuchehr A 2019 *Comput. Math. Appl.* **77** 2821
[5] Diaz-de-Anda A, Pimentel A, Flores J, Morales A, Gutierrez L and Mendez-Sanchez R A 2005 *J. Acoust. Soc. Am.* **117** 2814
[6] Sharma B and Sun C T 2015 *J. Sandw. Struct. Mater.* **18** 50
[7] Yang X D, Cui Q Q, Qian Y J, Zhang W and Lim C W 2018 *Journal of Applied Mechanics* **85** 061012
[8] Peiró-Torres M P, Castiñeira-Ibáñez S, Redondo J and Sáchez-Pérez J V 2019 *Appl. Phys. Lett.* **114** 171901
[9] Wang Y Z and Li F M 2012 *Chin. Phys. Lett.* **29** 034301
[10] Xu Y L, Chen C Q and Tian X G 2013 *Chin. Phys. Lett.* **30** 044301
[11] Yu D L, Liu Y Z, Wang G, Zhao H G and Qiu J 2006 *J. Appl. Phys.* **100** 124901
[12] Yu D L, Liu Y Z, Zhao H G, Wang G and Qiu J 2006 *Phys. Rev. B* **73** 064301
[13] Xiao Y, Wen J H and Wen X S 2012 *Phys. Lett. A* **376** 1384
[14] Xiao Y, Wen J H, Yu D L and Wen X S 2013 *J. Sound Vib.* **332** 867
[15] Zhou W J, Wu B, Su Y P, Liu D Y, Chen W Q and Bao R H 2019 *Mech. Adv. Mater. Struct.* 1
[16] Chen J S, Sharma B and Sun C T 2011 *Compos. Struct.* **93** 2120
[17] Chen J S and Sun C T 2011 *J. Sandw. Struct. Mater.* **13** 391
[18] Chen J S and Huang Y J 2016 *Journal of Vibration and Acoustics* **138** 0410091
[19] Pai P F, Peng H and Jiang S 2014 *Int. J. Mech. Sci.* **79** 195
[20] Alamri S, Li B and Tan K T 2018 *J. Appl. Phys.* **123** 095111
[21] Li Q Q, He Z C, Li E and Cheng A G 2018 *Smart. Mater. Struct.* **27** 095015
[22] Li Q Q, He Z C, Li E and Cheng A G 2019 *J. Appl. Phys.* **125** 035104
[23] Huang K X, Shui G S, Wang Y Z and Wang Y S 2020 *Mech. Mater.* **148** 103497
[24] Wei Z D, Li B R, Du J M and Yang G 2016 *Chin. Phys. Lett.* **33** 044303
[25] Koo G H and Park Y S 1998 *J. Sound Vib.* **210** 53
[26] Sorokin S V and Ershova O A 2004 *J. Sound Vib.* **278** 501
[27] Sorokin S V and Ershova O A 2006 *J. Sound Vib.* **291** 81
[28] Shen H J, Wen J H, Yu D L and Wen X S 2009 *J. Sound Vib.* **328** 57
[29] Shen H J, Wen J H, Yu D L and Wen X S 2009 *Acta. Phys. Sin.* **58** 8357 (in Chinese)
[30] Shen H J, Wen J H, Yu D L, Asgari M and Wen X S 2013 *J. Sound Vib.* **332** 4193
[31] Shen H J, Païdoussis M P, Wen J H, Yu D L and Wen X S 2014 *J. Sound Vib.* **333** 2735
[32] Shen H J, Wen J H, Yu D L, Yuan B and Wen X S 2014 *J. Fluid Structure* **46** 134
[33] Liang F and Yang X D 2020 *Appl. Math. Model* **77** 522
[34] Sorokin S and Holst-Jensen O 2012 *Journal of Vibration and Acoustics* **134** 041003
[35] Wang Y Z, Cui H T, Li F M and Kishimoto K 2011 *Phys. Lett. A* **375** 2448
[36] Yu D L, Wen J H, Zhao H G, Liu Y Z and Wen X S 2008 *J. Sound Vib.* **318** 193
[37] Yu D L, Wen J H, Zhao H G, Liu Y Z and Wen X S 2011 *Journal of Vibration & Acoustics* **133** 014502
[38] Yu D L, Wen J H, Shen H J and Wen X S 2012 *Phys. Lett. A* **376** 3417
[39] Yu D L, Païdoussis M P, Shen H J and Wang L 2014 *J. Appl. Mech.* **81** 011008
[40] Yu D L, Du C Y, Shen H J, Liu J W and Wen J H 2017 *Chin. Phys. Lett.* **34** 076202
[41] Yu D L, Shen H J, Liu J W, Yin J F, Zhang Z F and Wen J H 2018 *Chin. Phys. B* **27** 064301
[42] Wen J H, Shen H J, Yu D L and Wen X S 2010 *Chin. Phys. Lett.* **27** 114301
[43] Shen H J, Wen J H, Yu D L and Wen X S 2011 *IEEE International Conference on Mechatronics and Automation*, 7–10 Aug. 2011, p. 1700
[44] Iqbal M, Jaya M M, Bursi O S, Kumar A and Ceravolo R 2020 *Sci. Rep.* **10** 85
[45] Khudayarov B A, Komilova K M and Turaev F Z 2019 *International Journal Of Applied Mechanics* **11** 1950090
[46] Khudayarov B A, Komilova K M, Turaev F Z and Aliyarov J A 2020 *Int. J. Pressure Vessels Piping* **179** 104034
[47] Liu J W, Yu D L, Zhang Z F, Shen H J and Wen J H 2019 *Acta. Mech. Solida Sinica* **32** 173
[48] Qian Q, Wang L and Ni Q 2009 *Mech. Res. Commun.* **36** 413
[49] Gu J J, Dai B, Wang Y, Li M J and Duan M L 2017 *Ships and Offshore Structures* **12** 262
[50] Khudayarov B A, Komilova K M and Turaev F Z 2020 *Journal of Natural Gas Science And Engineering* **75** 103148